Pol. J. Environ. Stud. Vol. 33, No. 1 (2024), 443-454
DOI: *10.15244/pjoes/170852* ONLINE PUBLICATION DATE: 2023-12-06

Original Research

Properties of Binary and Ternary Blended Cement Containing Pond Ash and Ground Granulated Blast Furnace Slag

D Velumani[1]*, P Mageshkumar[2], K Yuvaraj[3]

[1]Department of Civil Engineering, Kamaraj College of Engineering & Technology, K.Vellakulam- 625 701, Tamilnadu, India
[2]Department of Civil Engineering, K.S.Rangasamy College of Technology, KSR Kalvi Nagar, Tiruchengode- 637 215, Tamilnadu, India
[3]Department of Civil Engineering, K.S.Rangasamy College of Technology, KSR Kalvi Nagar, Tiruchengode- 637 215, Tamilnadu, India

Received: 21 June 2023
Accepted: 8 August 2023

Abstract

Fly ash is a fine powdery particle collected from the unit operations of coal combustion furnaces in thermal power plants. Retained fly ash at bottom of hopper has been mixed with water and dumped in lagoons in form of slurry as pond ash (PA) or lagoon ash. Ground Granulated Blast Furnace Slag (GGBS) is a by-product obtained from steel industry. In this study, three phase of concrete specimens were prepared. In first phase, the specimens were prepared using 100% cement with various water-to-cementitious ratios. In second phase, specimens were prepared with varying water-to-cementitious ratios and PA contents ranging from 0 to 20%. Finally, the third phase, specimens were prepared to determine the optimal PA content, with GGBS ranging from 0 to 25%. The mechanical and rheological properties of different proportions of PA and GGBS have been experimentally investigated at 28 days. In addition, the flow ability and packing density of different proportions of PA and GGBS various mixes were tested. The test results revealed that combination of PA and GGBS up to 27% would enhance the fresh and harden properties of cementitious material. The rheological behaviour of optimal PA and GGBS concrete were tested at 28 days using scanning electron microscope (SEM). The results confirmed that the addition of PA and GGBS resulting in a denser, less porous, and more compact CSH microstructure in concrete.

Keywords: cementitious material, flow ability, packing density, strength properties, Rheology properties

*e-mail: velumani.se@gmail.com

Introduction

In the construction arena, concrete is construed as an inevitable construction material. Owing to infrastructure development, need for the concrete increases in the each passing year [1]. Currently production of sustainable concrete becomes a great challenge since the ingredient of concrete derived from the non-renewable geological sources [2]. Utilization of industrial by-products as a concrete ingredient is an ideal solution to overcome this problem [3, 5]. Now-a-days, enormous quantity of combustion by-products has been produced from thermal power plants. Fly ash (FA) is the major by-product obtained from the coal burning process [6]. Worldwide the annual production of FA is much higher than its consumption [7, 9]. Only 80% of the produced coal combustion by-products have been utilized and the residual ash has been disposed in ash ponds. The most insidious component formed simultaneously with FA is pond ash [10, 13].

Pond ash (PA) are alumino-silicate light weight free flowing particles. The density of PA range between 2000-2100 kg/m^3 [14]. Owning to their low density, pond ash (PA) in dry form can be easily carried by air and water [15]. Entrainment of ash in air may cause cardiovascular, respiratory problems to humans and animals [16, 18]. If it enters in to water bodies, it may harm aquatic livings [19]. Improper disposal of PA pose severe threat to environment. Hence this by-product should be disposed or reused in an effective manner [20, 21]. PA having cementitious properties, instead of disposing it as a waste material, it can be considered as a valued industrial by-product and used as a supplementary cementitious material (SCM) [22, 25]. PA produced by the thermal power plants consists of water holding capacity of 62-65% which plays a key role in enriching strength properties of the cement paste in concrete by according to standards [26].

By and large, the rheological properties mainly depend on the flow ability, which is significantly influenced by the supplementary cementitious material content and water/cementitious materials ratio [27, 29]. Packing density is one of the key parameter in the assessment of the flow ability of the cement mantle, particularly at low water-to-cementitious ratio [30, 32]. Higher packing density tends to and increases the free water content which lubricates the particles to produce water film coating. Hence, higher packing density could lead to a better workability [33, 35].

GGBS is an effective pozzalanic material which imparts good strength and flowability properties to the concrete. Enormous quantity of GGBS is produced in ferro silicon manufacturing industries as by-product [36]. In the production of green concrete, GGBS plays a substantial role. GGBS can also be employed as an effective substitute for cement in concrete to reduce the consumption of cement [37]. While using GGBS, considerable quantity of CO_2 emission can be reduced which helps to reduce global warming. Hence usage of GGBS has umpteen benefits in production of eco-friendly concrete [38, 40].

Pond ash is comprised of a slurry mixture containing a notable proportion of bottom ash and fly ash [41]. Pond ash consists of particles that can be categorized into coarser and finer fractions. The coarser fraction exhibits limited pozzolanic reactivity, while the finer fraction possesses stronger and more pronounced pozzolanic properties [42]. To harness its pozzolanic properties, pond ash is transformed into a fine powder through a pulverizing process [43]. Incorporating 10% ground pond ash as a substitute for cement can improve the strength characteristics of the material while simultaneously reducing carbon dioxide (CO_2) emissions [44, 45].

The strength of concrete mainly influenced by the rheological performance of cementitious materials [46]. Water retaining ability of the pozzolanic material could considerably condense the water requirements and enrich the strength properties of thecement paste in the concrete. However, sufficient water should be present in the mix to reduce the voids otherwise air may entrain through unfilled voids and the strength may be reduced [47, 48]. Few researchers reported that incorporation of optimal percentage of fine PA and GGBS particles would escalate the strength of concrete [49, 50]. Due to low density, good acoustic properties and thermal insulation, PA and GGBS have been preferred as a supplementary cementitious material [51]. Experimental investigations have been carried to assess the impact of PA and GGBS on the mechanical and rheological behaviour of the cement paste and results are discussed.

Materials

Ordinary Portland cement (OPC), PA and GGBS were used to produce cubes. OPC confirming grade 53 has been used. The specific surface area and specific gravity of OPC, PA and GGBS tested and found to be 325 m^2/kg and 3.14, 398 m^2/kg and 2.71 and 455 m^2/kg and 2.87 respectively. The chemical compositions of OPC, PA and GGBS are revealed in Table 1.

M-Sand, a manufactured sand, was utilized as the fine aggregate, while crushed blue granite metal was employed as the coarse aggregate for all the mixes. The specific gravity of M-sand and Blue granite metal found to be 2.71 and 2.69. The bulk density of M-sand and Blue granite metal are determined and found to be 1850 kg/m^3 and 1695 kg/m^3. Conplast SP430 super plasticizer is used in this study. The optimal dosage of super plasticizer was found to be 0.5% by mass of the cement.

Table 1. Chemical composition of the OPC and pond ash.

Constituent	Proportions (%)		
	OPC	Pond ash	GGBS
CaO	64.9	0.89	37.01
SiO_2	21.1	51.2	31.83
Al2O3	4.2	29.3	14.6
Fe_2O_3	3.9	7.64	3.81
MgO	2.5	0.87	8.7
Na_2O	0.8	1.9	-
SO_3	1.7	4.28	2.5
LOI	0.9	4.01	1.55

Mix Proportions

The mix proportions were formulated in accordance with the M20 grade specifications outlined in the Bureau of Indian Standards (BIS) of 2019 [52]. Experiments have been conducted in three phases as provided in Table 2. In the first phase, control mix with 100% OPC. In the second phase, PA content was varied from 0% to 20% in increments of 4% by the mass of cement. In addition, the third phase, optimum PA and GGBS content was varied from 0% to 25% in increments of 5% by the mass of cement. In this study, the water-to-cementitious ratios has been varied between 0.36 to 0.4 in increments of 0.2 by weight of cement.

Methods

Flow ability of the mix was assessed by Cone flow test. Fig. 1 shows the mini slump cone used for flow test. Cubical and split and flexural samples of size 150 mm x 150 mm x 150 mm ; 150 mm x 300 mm; 500 mm x 100 mm x 100 mm were used to assess the strength properties. SEM was carried out in the PSG institute of advanced studies, Coimbatore. Sample were prepared and tested as per BIS 516-1959 [26].

Results and Discussions

Compressive Strength

Binary Blended Concrete (BBC) and Ternary Blended Concrete (TBC)

Concrete cubes comprising various proportions of pond ash (PA) have been calculated at 28 days.

Table 2. Mix Proportions.

Mix	w/cm	Mixtures						
		OPC (Kg/m^3)	Pondash (Kg/m^3)	GGBS (Kg/m^3)	M-sand (Kg/m^3)	Coarseaggregate (Kg/m^3)	Water ($litre^3$)	Superplasticizer (%)
Phase - I	0.36	425.73	-	-	858.38	1092.5	153.26	0.5
	0.38	403.3			866.38	1103.2	153.26	
	0.40	383.15			874.06	1112.4	153.26	
Phase - II	0.36	408.71	17.02	-	858.38	1092.5	153.26	0.5
		391.68	34.05		858.38	1092.5	153.26	
		374.65	51.08		858.38	1092.5	153.26	
		357.62	68.11		858.38	1092.5	153.26	
		340.59	85.14		858.38	1092.5	153.26	
	0.38	387.17	16.13	-	866.38	1103.2	153.26	
		371.04	32.26		866.38	1103.2	153.26	
		354.91	48.39		866.38	1103.2	153.26	
		338.78	64.52		866.38	1103.2	153.26	
		322.64	80.66		866.38	1103.2	153.26	
	0.40	367.83	15.32	-	874.06	1112.4	153.26	
		352.5	30.65		874.06	1112.4	153.26	
		337.18	45.97		874.06	1112.4	153.26	
		321.30	61.30		874.06	1112.4	153.26	
		306.52	76.63		874.06	1112.4	153.26	

Table 2. Mix Proportions.

Phase - III	0.36	355.92	51.08	18.73	858.38	1092.5	153.26	0.5
		337.46		37.46	858.38	1092.5	153.26	
		318.46		56.19	858.38	1092.5	153.26	
		299.72		74.93	858.38	1092.5	153.26	
		280.99		93.66	858.38	1092.5	153.26	
	0.38	334.61	51.08	17.61	866.38	1103.2	153.26	
		317		35.22	866.38	1103.2	153.26	
		299.39		52.83	866.38	1103.2	153.26	
		281.78		70.44	866.38	1103.2	153.26	
		264.17		88.05	866.38	1103.2	153.26	
	0.40	315.47	51.08	16.60	874.06	1112.4	153.26	
		298.87		33.20	874.06	1112.4	153.26	
		282.07		50	874.06	1112.4	153.26	
		265.66		66.41	874.06	1112.4	153.26	
		249.06		83.01	874.06	1112.4	153.26	

*Phase - I - Control Mix (CM) ; Phase -II - Binary Blended Concrete (BBC); Phase - III - Ternary Blended Concrete(TBC)

Fig. 2 comprise the compressive strength of concrete cubes with variations of different mixes. Test results exhibited that the optimal replacement percentageof PA found to be 12%. Reduction in water-to-cementitious ratios considerably enhanced the cubes compressive strength up to 12% addition of PA. A lower water-cement ratio is associated with increased compressive strength in concrete [53]. It was observed that increasing the percentage of PA content beyond 12% tends to reduce the compressive strength. Hence, incorporation of PA up to 12% together with lower water-to-cementitious ratios would increase the strength. The lower value indicates the presence of unburned carbonpresent in the PA [43]. Higher strength attainment is due to thicker shell and the pozzolanic effect of the PA particles in the cementitious system.

The optimal percentage of PA content has been considered and the rest of the cementitious content was partially replaced with GGBS. Concrete cubes comprising different proportions of GGBS with optimal percentage of PA have been calculated at 28 days and shown in Fig. 3. 15% replacement of GGBS with cement along optimal percentage of PA gained higher compressive strength. The inclusion of GGBS in concrete leads to a more compact microstructure within the concrete matrix, thereby improving its strength [54].

Split Tensile Strength

Binary Blended Concrete (BBC) and Ternary Blended Concrete (TBC)

The split strength of concrete incorporating PA was evaluated and compared with the control mix at 28 days, as illustrated in Fig. 4. The 12% of PA concrete exhibited maximum split tensile strengths of 3.69 MPa, 3.79 MPa, and 3.88 MPa. Except for mix 16% and 20%

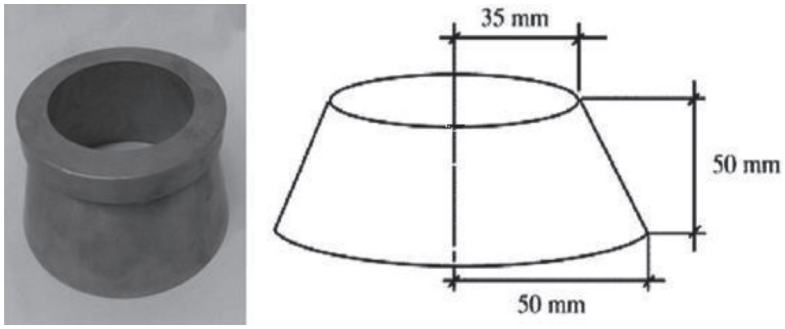

Fig. 1. Mini slump cone used for flow test.

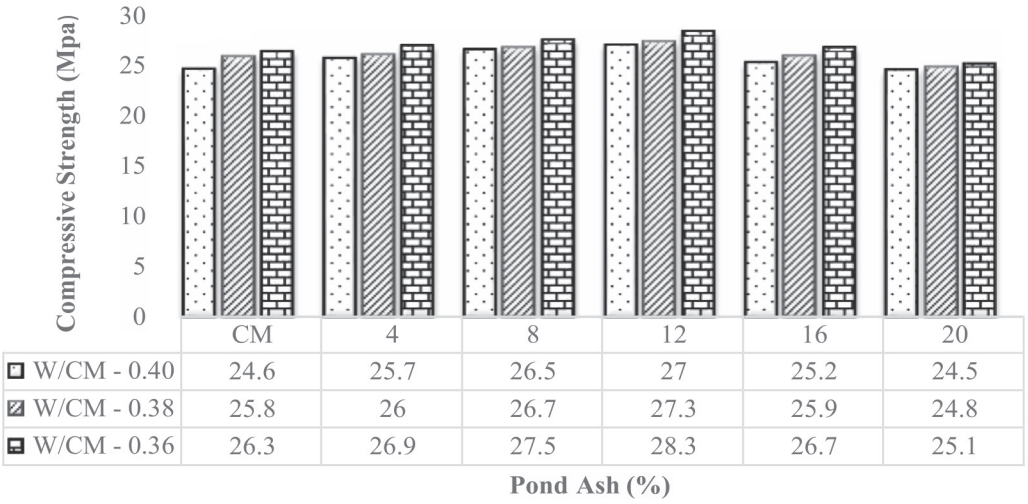

	CM	4	8	12	16	20
W/CM - 0.40	24.6	25.7	26.5	27	25.2	24.5
W/CM - 0.38	25.8	26	26.7	27.3	25.9	24.8
W/CM - 0.36	26.3	26.9	27.5	28.3	26.7	25.1

Fig. 2. Compressive strength Vs Pond ash content.

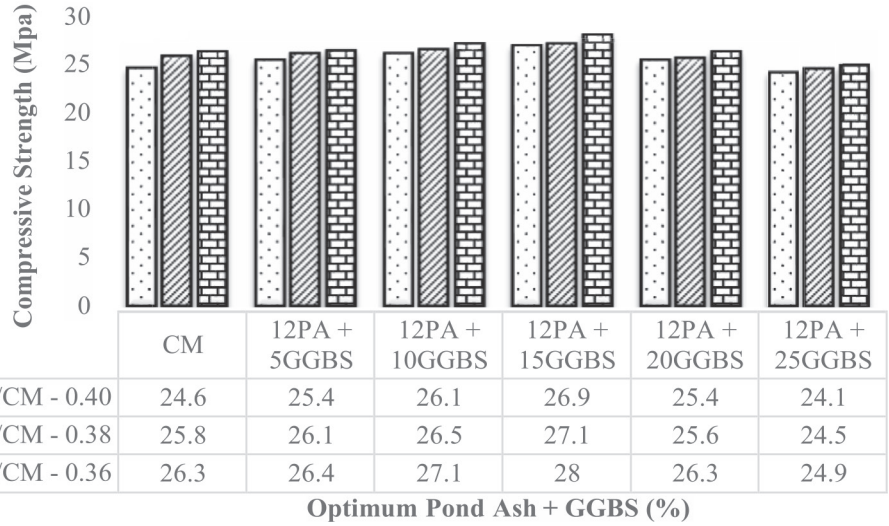

	CM	12PA + 5GGBS	12PA + 10GGBS	12PA + 15GGBS	12PA + 20GGBS	12PA + 25GGBS
W/CM - 0.40	24.6	25.4	26.1	26.9	25.4	24.1
W/CM - 0.38	25.8	26.1	26.5	27.1	25.6	24.5
W/CM - 0.36	26.3	26.4	27.1	28	26.3	24.9

Fig. 3. Compressive strength Vs Optimum pond ash with GGBS content.

of PA, the split tensile strength of PA concrete is higher compared to control mix.

Fig. 5 shows the Split tensile strength variations of different mixes incorporated with PA and GGBS. 15% GGBS found to be optimal replacement percentage for cement with PA. The 12 of PA with 15 of GGBS concrete exhibited maximum split tensile strengths of 3.75 MPa, 3.89 MPa, and 3.94 MPa. The inclusion of higher specific surface area and addition of calcium and silica in concrete are tends to improve the pozzolanic reaction of cement paste [55].

Flexural Strength

Binary Blended Concrete (BBC) and Ternary Blended Concrete (TBC)

The flexural strength of PA incorporated concrete takes into account and compared with control mix at 28 days as shown in Fig. 6. The scenario of instability in maintaining the flexural strength with gradual reduction of cement in the concrete matrix can be interpreted as follows: In case of OPC replacement with 12% of PA results in the flexural strength increase with standard curing times. The 12 of PA concrete exhibited maximum flexural strength of 5.49 MPa, 5.6 MPa, and 5.76 MPa. Except for mix 16% and 20% of PA, the flexural strength of PA concrete is higher compared to control mix.

Fig. 7 shows the flexural strength variations of different mixes incorporated with PA and GGBS. 15% GGBS found to be optimal replacement percentage for cement with PA. The12 of PA with 15 of GGBS concrete exhibited maximum flexural strengths of 5.42 MPa, 5.65MPa, and 5.75 MPa.

Packing Density and Void Ratio

Packing density (PD) and void ratio (VR) of the optimum PA with different proportions of GGBS added

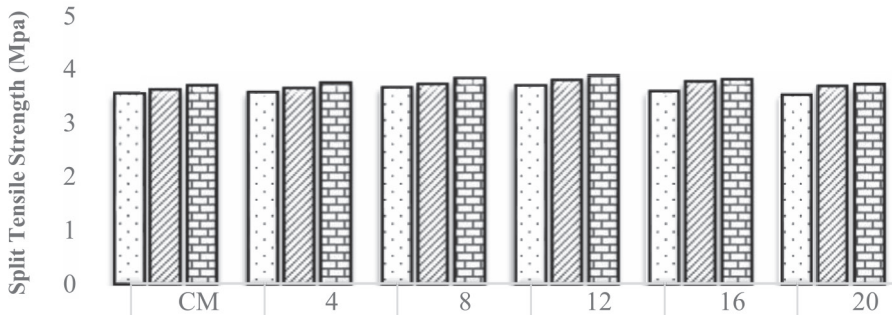

	CM	4	8	12	16	20
W/CM - 0.40	3.54	3.57	3.65	3.69	3.58	3.51
W/CM - 0.38	3.61	3.64	3.71	3.79	3.76	3.68
W/CM - 0.36	3.69	3.74	3.82	3.88	3.8	3.72

Pond Ash (%)

Fig. 4. Split tensile strength Vs pond ash content.

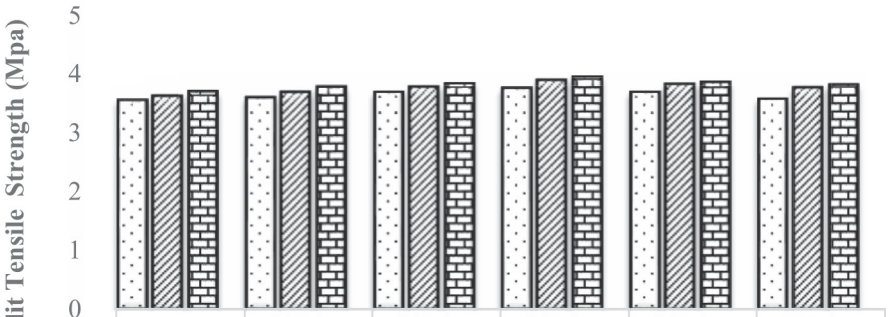

	CM	12PA + 5GGBS	12PA + 10GGBS	12PA + 15GGBS	12PA + 20GGBS	12PA + 25GGBS
W/CM - 0.40	3.54	3.59	3.68	3.75	3.68	3.57
W/CM - 0.38	3.61	3.68	3.77	3.89	3.82	3.76
W/CM - 0.36	3.69	3.77	3.83	3.94	3.85	3.81

Optimum Pond Ash with GGBS (%)

Fig. 5. Split tensile strength Vs Optimum pond ash with GGBS content.

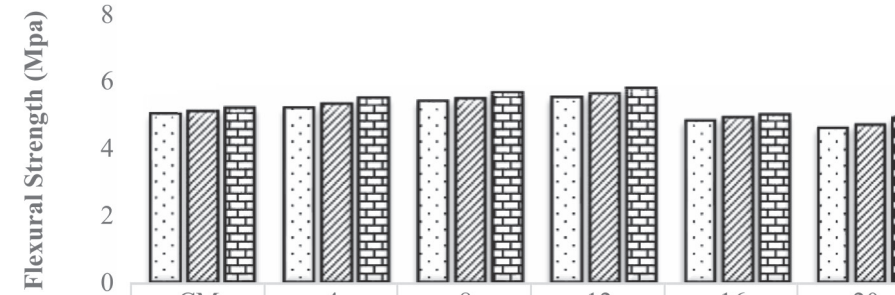

	CM	4	8	12	16	20
W/CM - 0.40	5	5.18	5.38	5.49	4.8	4.58
W/CM - 0.38	5.08	5.3	5.46	5.6	4.89	4.67
W/CM - 0.36	5.18	5.48	5.63	5.76	4.98	4.87

Pond Ash (%)

Fig. 6. Flexural strength Vs Pond ash content.

mixes have been calculated. The different water-to-cementitious ratios is essential to determine the packing density. Hence, three different water cement ratios (0.36 to 0.40) have been used in this study. The bulk densities of the mixes for different ratios were calculated to find the solid concentrations.

Generally, if the percentage of water increases, the solid concentration would reach a peak value and then decline. The maximum solid concentration value ρ_{max} was taken as the packing density [17]. Fig. 8 shows the packing density variations of cementitious suspension comprising optimum PA with different proportions of GGBS for different water-to- cementitious ratios. Test results indicated that incorporation of TBC considerably increases the PD than CM at all water-to-cementitious ratios. Increasing trend in PD was observed up to 15% replacement in TBC at different water-to-cementitious ratios. Sample PA12+15GGBS obtained higher PD of 0.74 among all the samples tested. At different water- to-cementitious ratios, beyond 15% replacement of TBC, the PD slightly declined to 0.65 and 0.63; 067 and 0.65 and 0.72 and 0.71 for the samples PA12+20GGBS and PA12+25GGBS respectively.

Based on results obtained from the PD test, the voids ratio E (volume of voids to the volume of solid) and the excess water ratio E' (excess water to solid volume ratio) have been calculated as and mentioned in Equ. (1) and Equ. (2):

$$E = (1-\rho max)/\rho max \quad (1)$$

$$E' = E_w - E \quad (2)$$

E_w represents water to solid ratio of the cement paste. E' is the quantity of excess water in the cement paste per solid volume of the cementitious materials [17]. Variations in the voids ratios of the TBC

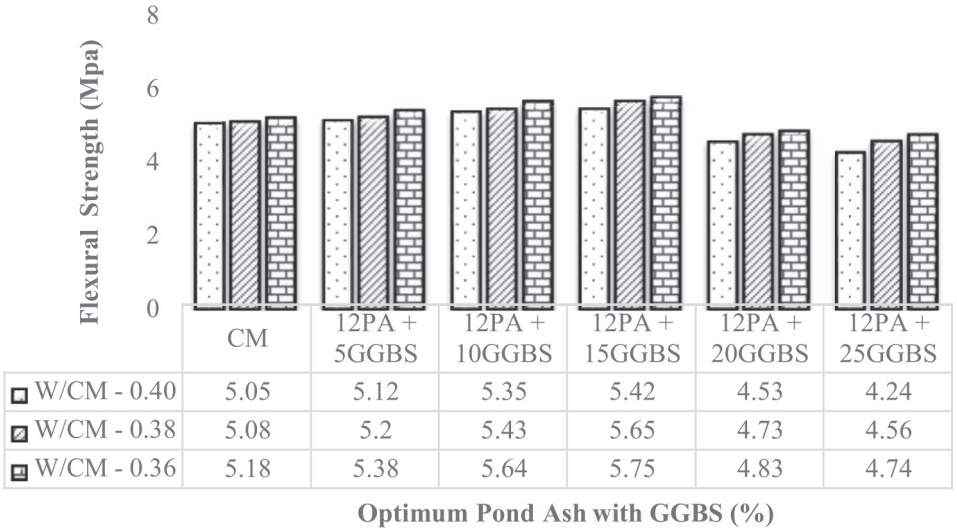

	CM	12PA + 5GGBS	12PA + 10GGBS	12PA + 15GGBS	12PA + 20GGBS	12PA + 25GGBS
W/CM - 0.40	5.05	5.12	5.35	5.42	4.53	4.24
W/CM - 0.38	5.08	5.2	5.43	5.65	4.73	4.56
W/CM - 0.36	5.18	5.38	5.64	5.75	4.83	4.74

Fig. 7. Flexural strength Vs Optimum pond ash with GGBS content.

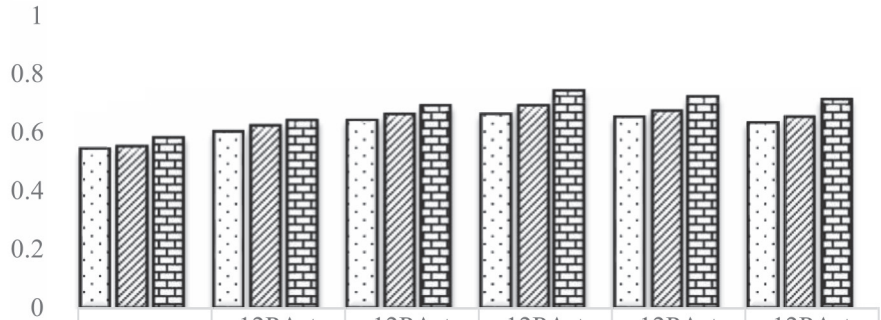

	CM	12PA + 5GGBS	12PA + 10GGBS	12PA + 15GGBS	12PA + 20GGBS	12PA + 25GGBS
W/CM - 0.40	0.54	0.6	0.64	0.66	0.65	0.63
W/CM - 0.38	0.55	0.62	0.66	0.69	0.67	0.65
W/CM - 0.36	0.58	0.64	0.69	0.74	0.72	0.71

Fig. 8. Packing density variations of samples with ternary concrete.

mixes are shown in Fig. 9. Test results confirmed that the incorporation of PA considerably minimized the voids ratio of the cement paste than CM.

Associating the PD variations with relevant VR, the higher increase in PD and reduction in the VR for the TBC. Higher reduction in VR considerably reduces the required quantity of water to fill the voids of cement paste and tends to enhance the free water content. Higher free water present in the cement paste would form water films around solid particles and improves lubrication [56, 57].

Flow Spread

Fig. 10 shows the flow spread variations of the mixes for TBC with water-to- cementitious ratios. Flow test results indicated that the flow spread increases with respect to water-to-cementitious ratios and PA and GGBS content of the mix. Highest flow rate obtained at water-to-cementitious ratios of 0.40. However, water-to-cementitious ratios are not a predominant factor which governs flow spread. Addition of 15% GGBS with 12% PA content escalates the flow spread 276 mm; whereas the flow spread value of the mix comprising 20% and 25% of GGBS with 12% PA found to be 291 and 297 mm. Slight increase in flow spread beyond 25 of GGBS with 12% PA may be due to less water film thickness which tends to restrict the flow ability of the mix.

Flow Rate

The flow time was calculated during the flow spread test and based on the obtained values the flow rate has been calculated. Fig. 11 shows the flow rate variations of the mixes for different GGBS with optimum PA content. Test results revealed that the increase in water-to-cementitious ratios increases the flow rate but water-to-cementitious ratios alone not a predominant factor which governs flow rate as like flow spread. Highest flow rate

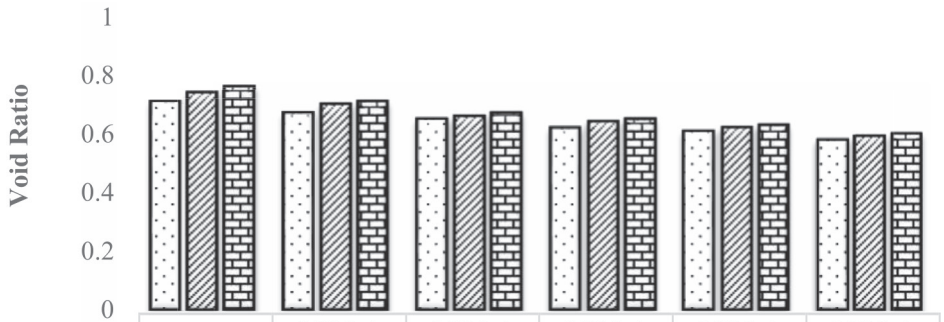

	CM	12PA + 5GGBS	12PA + 10GGBS	12PA + 15GGBS	12PA + 20GGBS	12PA + 25GGBS
W/CM - 0.40	0.71	0.67	0.65	0.62	0.61	0.58
W/CM - 0.38	0.74	0.7	0.66	0.64	0.62	0.59
W/CM - 0.36	0.76	0.71	0.67	0.65	0.63	0.6

Fig. 9. Void ratio variations of samples with TBC.

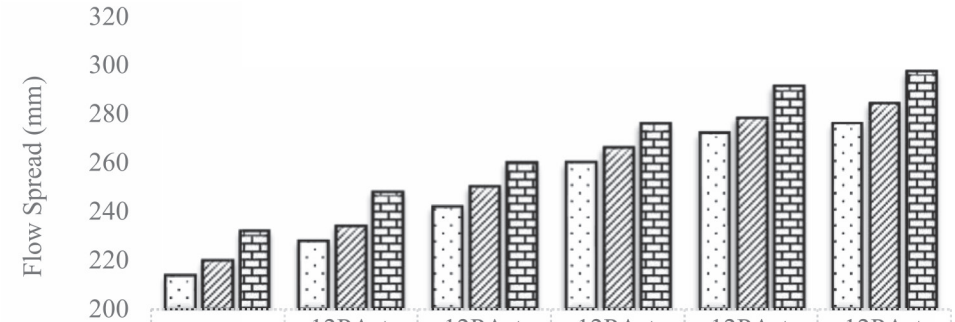

	CM	12PA + 5GGBS	12PA + 10GGBS	12PA + 15GGBS	12PA + 20GGBS	12PA + 25GGBS
W/CM - 0.36	214	228	242	260	272	276
W/CM - 0.38	220	234	250	266	278	284
W/CM - 0.40	232	248	260	276	291	297

Fig. 10. Flow spread of mixes for TBC with different water-to-cementitious ratios.

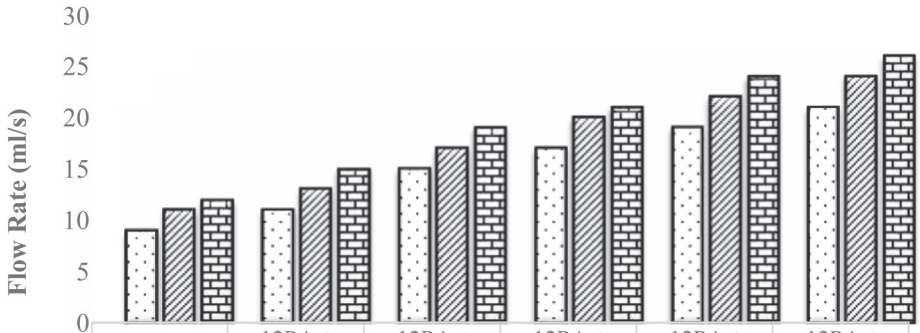

	CM	12PA + 5GGBS	12PA + 10GGBS	12PA + 15GGBS	12PA + 20GGBS	12PA + 25GGBS
W/CM - 0.36	9	11	15	17	19	21
W/CM - 0.38	11	13	17	20	22	24
W/CM - 0.40	12	15	19	21	24	26

Fig. 11. Flow rate of mixes for different W/CM ratios.

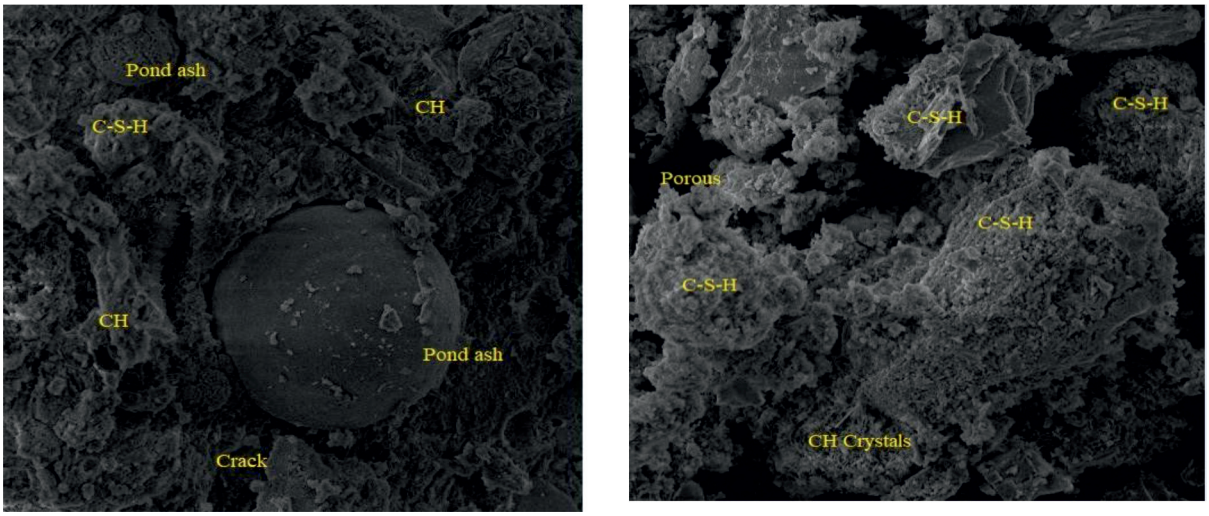

Fig. 12. SEM image of CM and 12PA+15GGBS.

was obtained at water-to-cementitious ratio of 0.40 and the flow rate flow rate has significantly improved for the all the mixes than CM. At w/cm of 0.40, the CM had a lower flow rate of 12ml/s and 12PA with 25% of GGBS had a higher flow rate of 26 ml/s.

Micro Structure Properties

The SEM analysis of CM and 12PA+15GGBS concrete samples after 28 days of curing is depicted in Fig. 12. Calcium–Silica–Hydrate (C–S–H) is the major component found in the concrete matrix of 12PA + 15GGBS mix concrete than CM. The key factors influencing the formation of C–S–H gel are: morphology and particle distribution of ingredients, concentration and orientation of particles, composition and pore structure of the phases [58]. The un reacted PA particle and porous space was observed in CM at 28 days, due to delay of primary hydration [59]. The SEM analysis reveals a denser microstructure in 12PA+15GGBS concrete samples after 28 days of curing, characterized by the depletion of Portlandite (CH) crystals and the presence of additional calcium silicate hydrate gel. At 28 days, the 12PA+15GGBS mix clearly demonstrates a reduced presence of CH crystals compared to CM.

Conclusion

The experimental investigation on influence of PA and GGBS on cementitious suspensions has been conducted and the following conclusions are drawn:

– Mix PA12+15GGBS obtained highest compressive, split tensile and flexural strength value of 28.3, 3.94 and 5.75 MPa respectively. Test results revealed that the optimal replacement percentage of PA and GGBS with OPC is 27%.
– Test results evident that PA12+15GGBS mix content could increase the packing density. Addition of PA and GGBS up to 12% and 15% respectively

considerably increased the packing density and beyond 15% GGBS addition, slight decrease in packing density was observed.
– For 15% addition of GGBS with 12% PA at water-to-cementitious ratio of 0.40, the packing density increase found to be 18.9% than the control mix and the corresponding void ratio reduction found to be 43.7%.
– Increase in GGBS content improved the flow spread of the mixes. Mix PA12+15GGBS obtained flow spread of 276 mm. Further, better improvement in flow rate was obtained for the mix PA12+15GGBS. Increase in PA content and water- to-cementitious ratio considerably improved the flow rate of all the mixes.
– The incorporation of PA12+15GGBS mix concrete leads to the development of a more compact matrix as a result of reduced (CH) crystal content and enhanced formation of CSH paste. Moreover, SEM analysis clearly indicated that the inclusion of PA with GGBS in concrete does not affect the bonding characteristics of the concrete during hydration.

PA with GGBS have been proved as a prominent material for improving the rheology, particle packing and mechanical properties of the cementitious suspension. Utilization of PA with GGBS substantially reduces the cement consumption and endorses sustainable development.

Conflict of Interest

The authors declare no conflict of interest.

References

1. ALQAMISH H.H., AL-TAMIMI A.K. Development and Evaluation of Nano-Silica Sustainable Concrete. Applied Sciences, **11** (7), 3041, **2021**.
2. GADORE V., AHMARUZZAMAN M. Tailored fly ash materials: A recent progress of their properties and applications for remediation of organic and inorganic contaminants from water. Journal of Water Process Engineering, **41**, 101910, **2021**.
3. BROOKS A.L., FANG Y., SHEN Z., WANG J., ZHOU H. Enabling high-strength cement-based materials for thermal energy storage via fly-ash cenosphere encapsulated phase change materials. Cement Concrete Composites, **120**, 104033, 2021.
4. NITHYANANDAM A., DEIVARAJAN T. Development of fly ash cenosphere based composite for thermal insulation application. International Journal of Applied Ceramic Technology, **18**, 1825, **2021**.
5. UJJWAL SHARMA A.C., NAKUL GUPTA A., KULDEEP K.S. Comparative study on the effect of industrial by-products as a replacement of cement in concrete. Materials Today: Proceedings, **44** (1), 45, **2021**.
6. HAUSTEIN E., KURYŁOWICZ-CUDOWSKA A. The Effect of Fly Ash Microspheres on the Pore Structure of Concrete. Minerals, **10** (1), 58, **2020**.
7. BAI Y., DARCY F., BASHEER P.A.M. Strength and drying shrinkage properties of concrete containing furnace bottom ash as fine aggregate. Construction and Building Materials, **19**, 691, **2005**.
8. DANISH A., MOSABERPANAH M.A. Formation mechanism and applications of cenospheres: A review. Journal of Materials Science, **55**, 4539, **2020**.
9. SATPATHY H.P., PATEL S.K., NAYAK A.N. Development of sustainable lightweight concrete using fly ash cenosphere and sintered fly ash aggregate. Construction and Building Materials, **202** (2), 636, **2019**.
10. YORIYA S., INTANA T., TEPSRI P. Separation of Cenospheres from Lignite Fly Ash Using Acetone–Water Mixture. Applied Sciences, **9** (18), 3792, **2019**.
11. STRZAŁKOWSKA E. Morphology, chemical and mineralogical composition of magnetic fraction of coal fly ash. International Journal of Coal Geology, **240**, 103746, **2021**.
12. KUSHNOORE S., KAMITKAR N., ATGUR V., UPPIN M.S., SATISHKUMAR M. A Review on Utilization of Light Weight Fly Ash Cenosphere as Filler in both Polymer and Alloy-Based Composites. Journal of Mechanical Engineering Research, **3**, 17, **2020**.
13. AGRAWAL U., WANJARI S. Physiochemical and engineering characteristics of cenosphere and its application as a lightweight construction material – A review. Materials Today: Proceedings, **4**, 9797, **2017**.
14. ADESINA A. Sustainable application of cenospheres in cementitious materials – Overview of performance. Developments in the Built Environment, 4, 100029, **2020**.
15. HANIF A., LU Z., LI Z., Utilization of Fly Ash Cenosphere as lightweight filler in Cement-Based Composites – A Review, Construction and Building Materials, **144**, 373, **2017**.
16. IS12269: **2013**. Indian Standards Ordinary Portland Cement, 53 Grade specifications.
17. KWAN A.K.H., CHEN J.J. Adding fly ash microsphere to improve packing density, flowability and strength of cement paste, Powder Technology, **234**, 19, **2013**.
18. FENELONOV V.B., MEL'GUNOV M.S., PARMON V. The Properties of Cenospheres and the Mechanism of Their Formation During High-Temperature Coal Combustion at Thermal Power Plans, Powder and Particle, **28**, 189, **2010**.
19. FOMENKO E.V., ANSHITS N.N., PANKOVA M.V., SOLOVYOV L.A., ANSHITS A.G. Fly Ash Cenospheres: composition, Morphology, Structure, and Helium Permeability, World Coal Ash Conference, May 9-12, 2011, Denver, CO, USA, **2011**.
20. HANIF A., DIAO S., LU Z., FAN T., LI Z. Green lightweight cementitious composite incorporating aerogels and fly ash cenospheres – Mechanical and thermal insulating properties, Construction and Building Materials, **116**, 422, **2016**.
21. ZHOU H., BROOKS A.L., Thermal and mechanical properties of structural lightweight concrete containing lightweight aggregates and fly-ash cenospheres. Construction and Building Materials, **198**, 512, **2019**.
22. WANG J.Y., ZHANG M.H., LI W., CHIA K.S., LIEW J.Y.R. Stability of Cenospheres in Lightweight Cement Composites in Terms of Alkali-Silica Reaction, Cement and Concrete Research, **42**, 721, **2012**.
23. WANG C., LIU J., DU H., GUO A. Effect of fly ash cenospheres on the microstructure and properties of silica-based composites, Ceramics International, **38**, 4395, **2012**.

24. ASTM C1723-10. Standard Guide for Examination of Hardened Concrete Using Scanning Electron Microscope.
25. HANIF Z., LU Y., CHENG S., DIAO LI Z. Effects of different lightweight functional fillers for use in cementitious composites. International Journal of Concrete Structures and Materials. **11** (1), 99, **2017**.
26. IS 516:1959 (Reaffirmed 2004). Method of Tests for Strength of Concrete.
27. ARUNVIVEK G.K., RAMESHKUMAR D. Experimental Investigation on Performance of Waste Cement Sludge and Silica Fume-Incorporated Portland Cement Concrete. Journal of The Institution of Engineers (India): Series A, **100** (4), 611, **2019**.
28. LIU F., WANG J., QIAN X., HOLLINGSWORTH J. Internal curing of high performance concrete using cenospheres. Cement and Concrete Research, **95**, 39, **2017**.
29. SONG H., XIE W., LIU J., CHENG F., GASEM KA., FAN M. Effect of surfactants on the properties of a gas-sealing coating modified with fly ash and cement. Journal of Materials Science, **53** (21), 15142, **2018**.
30. SENTHAMARAI KANNAN K., ANDAL L., SHANMUGASUNDARAM M. An Investigation on Strength Development of Cement with Cenosphere and Silica Fume as Pozzolanic Replacement. Advances in Materials Science and Engineering, **2016**.
31. SOUTSOS M., GRUYAERT E. Properties of Fresh and Hardened Concrete Containing Supplementary Cementitious Materials. Springer link, 55, **2018**.
32. LIU F., WANG J., QIAN X. Integrating phase change materials into concrete through microencapsulation using cenospheres. Cement and Concrete Composites, **80**, 317, **2017**.
33. YRKOWSKI M., NETO R.C., SANTOS L.F., WITKOWSKI K. Characterization of fly-ash cenospheres from coal-fired power plant unit. Fuel, **174**, 49, **2016**.
34. FOMENKO E.V., ANSHITS N.N., SOLOVYOV L.A., MIKHAYLOVA O.A., ANSHITS A.G. Composition and Morphology of Fly Ash Cenospheres Produced from the Combustion of Kuznetsk Coal. Energy Fuels, **27** (9), 5440, **2013**.
35. YAO Z.T., JI X.S., SARKER P.K., TANG J.H., GE L.Q., XIA M.S., XI Y.Q. A comprehensive review on the application of coal fly ash, Earth-Science Reviews, **141**, 105, **2015**.
36. KRISTOMBU BADUGE S., MENDIS P., SAN NICOLAS R., NGUYEN K., HAJIMOHAMMADI, Performance of lightweight hemp concrete with alkali-activated cenosphere binders exposed to elevated temperature. Construction and Building Materials, **224**, 158, **2019**.
37. HU J. Comparison between the effects of superfine steel slag and superfine phosphorus slag on the long-term performances and durability of concrete. Journal of Thermal Analysis and Calorimetry, 128, 1251, **2017**.
38. AHMAD J., MARTÍNEZ-GARCÍA R., SZELAG M., DE-PRADO-GIL J., MARZOUKI R., ALQURASHI M., HUSSEIN E.E. Effects of Steel Fibers (SF) and Ground Granulated Blast Furnace Slag (GGBS) on Recycled Aggregate Concrete. Materials. **14**, 7497, **2021**.
39. HAJIMOHAMMADI A., NGO T., PROVIS J.L., KIM T., VONGSVIVUT J. High strength/density ratio in a syntactic foam made from one-part mix geopolymer and cenospheres. Composites Part B: Engineering, **173**, 106908, **2019**.
40. LO T.Y., W.C. TANG W.C., CUI H.Z The effects of aggregate properties on lightweight concrete, Building and Environment, **42**, 3025, **2007**.
41. YUVARAJ K., RAMESH S. Experimental investigation on strength properties of concrete incorporating ground pond ash. Cement wabno beton, **26** (3), 253, **2021**.
42. HALDIVE S.A., KAMBEKAR A.R. Experimental Study on Combined Effect of Fly Ash and Pond Ash on Strength and Durability of Concrete, International Conference on Innovations in Civil Engineering, 81-86, **2013**.
43. YUVARAJ K., RAMESH S., VELUMANI M. Predicting the mechanical strength of coal pond ash based geopolymer concrete using linear regression method. Materials today proceeding, **04**, 514, **2023**.
44. LOGANATHAN P., MOHANRAJ R., SENTHILKUMAR S., YUVARAJ K. Mechanical performance of ETC RC beam with U-framed AFRP laminates under a static load condition. Revista de la construcción, **21**, 678, **2022**.
45. YUVARAJ K., RAMESH S. A review on green concrete using low-calcium pond ash as supplementary cementitious material. International research journal of multidisciplinary technovation, **1** (6), 353, **2019**.
46. VEDIYAPPAN S., CHINNARAJ P.K., HANUMANTRAYA B.B., SUBRAMANIAN S.K. An Experimental Investigation on Geopolymer Concrete Utilising Micronized Biomass Silica and GGBS. KSCE Journal of Civil Engineering, **25**, 2134, **2021**.
47. RAAFIDIANI R., SUMARGO S., PERMANA R. The Influence of Ground Granulated Blast Furnace Slag (GGBFS) as Portland Composite Cement (PCC) Substitution in Improving Compressive Strength of Concrete. In Proceedings of the 5th Annual Applied Science and Engineering Conference (AASEC 2020), Bandung, Indonesia, 20–21, **1098**, 22035, April **2020**.
48. BHEEL N., ABBASI S.A., AWOYERA P., OLALUSI O.B., SOHU S., RONDON C., ECHEVERRÍA A.M. Fresh and Hardened Properties of Concrete Incorporating Binary Blend of Metakaolin and Ground Granulated Blast Furnace Slag as Supplementary Cementitious Material. Advances in Civil Engineering, 8851030, **2020**.
49. SOUZA F., MONTEDO O., GRASSI R., ANTUNES E.G.P. Lightweight high-strength concrete with the use of waste cenosphere as fine aggregate. Matéria, 24, **2019**.
50. SURESH D., NAGARAJU K. Ground Granulated Blast Slag (GGBS) In Concrete – A Review. Journal of Mechanical and Civil Engineering, **12**, 76, **2015**.
51. FRIGIONE M., LETTIERI M., SARCINELLA A. Phase Change Materials for Energy Efficiency in Buildings and Their Use in Mortars. Materials. **12**, 1260, **2019**.
52. BIS (Bureau of Indian Standards). Concrete mix proportioning – guidelines (Second Revision). New Delhi, **2019**.
53. KAN A., DEMIRBOGA R. A novel material for lightweight concrete production, Cement Concrete Composites, **31**, 489, **2009**.
54. LENKA B.P., MAJHI R.K., SINGH S., NAYAK A.N. Eco-Friendly and Cost-Effective Concrete Utilizing High-Volume Blast Furnace Slag and DemolitionWaste with Lime. European Journal of Environmental and Civil Engineering, 1, **2021**.
55. DHARMARA J.R., ARUNVIVEK G.K., ALAGAR KARTHIC K., MOHANVE L. Investigation on mechanical and durability properties of concrete mixed with water exposed to a magnetic field, Advances in Civil Engineering, **202**, 1, **2021**.
56. NG S., JELLE B.P., SANDBERG L.I.C., GAO T., WALLEVIK Ó.H. Experimental investigations of

aerogel-incorporated ultra-high performance concrete. Construction and Building Materials, **77**, 307, **2015**.
57. HENRY H. C. WONG., ALBERT K. H. KWAN., Packing density of cementitious materials: part 1 – measurement using a wet packing method Materials and Structures. **41**, 689, **2008**.
58. BURHAN U., ABDULKADIR C.A. Analysis of fly ash concrete with scanning electron microscopy and X-ray diffraction. Advances in Science and Technology Research Journal **13** (4), 100, **2019**.
59. CHANDRA SEKHAR K., RATHISH KUMAR P. The study of the microstructure of sustainable composite cement-based mortars. Cement Wapno Beton **25**, 390, **2020**.